A LIGHT SCATTERING STUDY OF TURBULENCE

W.I. GOLDBURG, P. TONG [1] and H.K. PAK

Department of Physics and Astronomy, University of Pittsburgh, Pittsburgh, PA 15260, USA

By scattering light from a turbulent fluid seeded with small particles, one obtains information about turbulent velocity fluctuations over varying spatial scales, R. The measured intensity autocorrelation function, $g(t)$, is related to the probability density $P(V(R))$ of finding velocity fluctuations of magnitude $V(R)$ associated with eddies of size R. The measurements described here strongly suggest that the energy-containing eddies occupy a fractal region whose dimension (or spectrum of dimensions) increases with the Reynolds number Re when Re exceeds some threshold value.

1. Introduction

In his seminal book, The Fractal Geometry of Nature, Benoit Mandelbrot [1] makes clear his deep interest in the geometrical nature of turbulence. As he points out, the description of the visual appearance of a turbulent fluid, such as smoke curling up from a cigarette, taxes our powers of description. It seems that present-day speech is not well suited to evoking the image of self-similar structures. After all, it takes a series of images, one magnified with respect to the other, to identify fractal structures. And turbulence is, by all evidence, a fractal thing at its roots[2].

There are many ways of revealing the fractal or spotty nature of a turbulent fluid. One technique is to measure the time variation of the square of the velocity at a point in the fluid [3]. Another is to add a small amount of long-chain molecules to the fluid and observe it through crossed polaroids [4]. The molecules are locally aligned by turbulent shear forces. These molecules, being anisotropic scatterers, depolarize the light in regions where the shear is large, making the local structure of the strong vorticity directly visible.

Herein we describe experiments, carried out at the University of Pittsburgh, which provide a new approach to the study of the small-scale structure of turbulence. The method involves a measurement of the autocorrelation function of the light intensity scattered by small particles suspended in the turbulent fluid. For this technique there is no need to invoke the "frozen turbulence assumption" to translate temporal information to spatial information. According to this assumption, small-scale eddies (the ones of interest), are transported past a velocity measuring device with the mean velocity U of the flow. If these small-scale eddies remain intact for a long enough time, a time record of the velocity $v(t)$ at a point will reveal spatial features of the flow through the equation $v(t) = v(x/U)$. The frozen turbulence assumption fails unless the velocity fluctuations $V(R)$ associated with eddies of size R are uncoupled from the larger-scale eddies.

The technique of photon correlation homodyne spectroscopy (HS) [5], which we have used in our experiments, is that of recording the beating of scattered light waves that have been Doppler shifted by pairs of particles seeded in the turbulent fluid. The technique was introduced many years ago by Bourke et al. [6], but seems largely to have been ignored. Being an optical technique, it permits non-invasive observation of velocity fluctuations at very small scales.

The homodyne scheme is readily understood from fig. 1, which shows two moving particles at a particular instant of time when their separation is R and their velocities are v_1 and v_2. The seed particles are small enough that they scatter light isotropically. A photodetector (PMT), located at an angle θ with respect to the incident beam, receives the light from both particles. The scattered light from each particle is Doppler shifted by an amount $k \cdot v_1$ and $k \cdot v_2$ respectively, where k is the scattering vector, of magnitude $k = (4\pi n/\lambda)\sin(\tfrac{1}{2}\theta)$. Here λ is the vacuum wavelength of the light ($\lambda = 488$ nm in our experiments), and n is the refractive index of the turbulent fluid; in our case the fluid was water. The photomultiplier, which receives the light from the particle pair, is a square-law detector, so that its output current, $I(t)$, contains a beating term proportional to $\cos[kV_k(R)t]$, where V_k is the projection of the velocity difference $v_1 - v_2$ along the direction of k. Henceforth the subscript on $V_k(R)$ will be dropped, but its R dependence will be retained.

The essential aspect of turbulence is that the velocity difference between two points in the fluid depends on the separation R of these two points. According to the theory of Kolmogorov [6], the moments of the velocity fluctuations $V(R)$ obey a scaling law

$$\langle V(R)^n \rangle \sim u(R)^n \sim R^{\xi_n}, \qquad (1)$$

with $\xi_n = \tfrac{1}{3}n$. The homodyne technique is well suited to measure the lower moments of $V(R)$, but not the higher moments. On the other hand, the method yields information about the functional form of the probability density $P(V(R))$, that two points in the fluid, separated by a distance R, have velocity difference lying within $V(R)$ and $V(R) + dV(R)$. Our central finding is that $P(V(R))$ is well represented by a Lorentzian function,

$$P(V(R)) \propto \{1 + [V(R)/u(R)]^2\}^{-1}, \qquad (2)$$

for relatively small values of $V(R)$. We also find that the scaling velocity $u(R) \sim R^\zeta$, where ζ is a function of Reynolds number, Re. The measurements were made at very modest values of the Reynolds number. In fact the turbulence was so weak that one might not have thought the flow would exhibit the self-similarity which was indeed observed. Throughout this paper the Reynolds number is defined as Re $= Ul_0/\nu$, where U is the mean velocity of the flow, l_0 is the outer scale of the turbulence, and ν is the kinematic viscosity of the fluid.
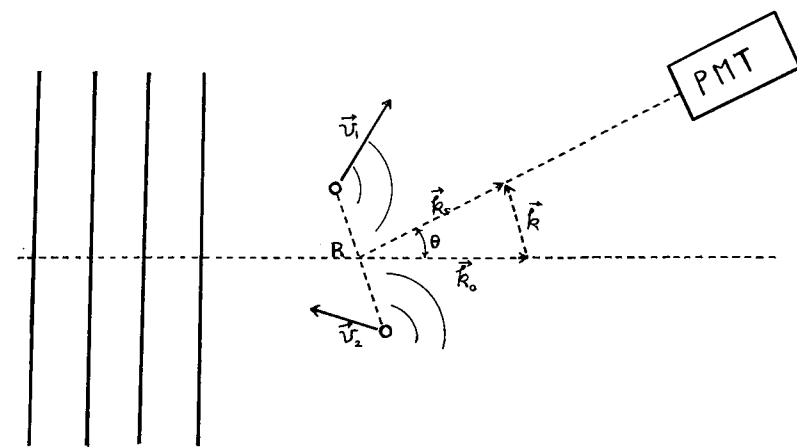

Fig. 1. A schematic diagram showing scattering geometry. The scattering vector $k = k_s - k_0$, where k_s and k_0 are the scattered and incident wave vectors respectively.

2. Experimental

The detailed experimental setup can be found in ref. [8]. The fluid flow was generated in a closed water tunnel comprised of a cylindrical pipe and a pump of variable speed. The turbulence is generated by a grid within the pipe. The grid can be removed to permit study of wall-generated turbulence (pipe flow). A baffle section placed in the high-pressure side of the grid, suppresses the turbulence generated by the pump and by those sections of pipe on the high-pressure side of the grid. With this arrangement all of the turbulence is generated by the grid only. In most of the experiments discussed here the diameter of the pipe was 4.4 cm, and the aperture size of the grid was 3.1 mm. These parameters are taken to be l_0 in calculating the Reynolds number. The measurements were made 28 cm downstream from the grid. The water which flowed through the pipe was seeded with polystyrene spheres 60 nm in diameter. These particles were small enough to scatter light isotropically and in sufficient concentration that their mean separation was much less than the Kolmogorov dissipation length l_d, which was estimated to be a fraction of a millimeter.

On the downstream side of the grid there is an optically transparent section of piping to admit the incident laser beam and observe the scattering. Because the flow is seeded, a thin column of the scattered light is produced in the water and that light is imaged with a lens, on a slit of variable width, L. By varying L, the homodyne scheme permits the probing of velocity fluctuations $V(R)$ from the smallest scale l_d to that of the width of the slit, L.

Using a standard light scattering apparatus and a digital correlator, we measure the intensity autocorrelation function, $g(t) = \langle I(t') I(t'+t)\rangle/\langle I(t')\rangle^2$, where $I(t)$ is the scattered light intensity measured at scattering angle θ, and the angle brackets represent a time average over t'. One can show [8] that the correlation function $g(t)$ has the following form:

$$g(t) = 1 + f(A) G(t) . \tag{3}$$

The geometrical factor $f(A)$ is of order unity if the

photodetector receives light from only one coherence area [5]. All of the interesting physics is contained in $G(t)$, which is proportional to a sum of the time-averaged phase factors $\cos(ktV)$ coming from the Doppler shift of all particle pairs in the scattering volume. The function $G(t)$ can be written as [8]

$$G(t) = \int_0^L dR \, h(R) \int_{-\infty}^{\infty} dV(R) \, P(V(R))$$
$$\times \cos[kV(R)t] , \tag{4}$$

where $h(R)$ is the probability of finding a particle pair, separated by R, in the columnar region of length L.

If the image on the slit is taken to be quasi-one-dimensional, which is valid when the slit width remains large compared to the diameter of the laser beam, $h(R) = 2(1 - R/L)/L$. Note that the inner integral in eq. (4) is the Fourier cosine transform of $P(V(R))$, and the $G(t)$ may be thought of as a transform of the characteristic function. If the probability density $P(V(R))$ has the scaling form $P(V(R)) = Q[V(R)/u(R)]/u(R)$, eq. (4) becomes

$$G(t) = \int_0^L dR \, h(R) \, F(ktu(R)) , \tag{5}$$

where F is the Fourier cosine transform of $Q[V(R)/u(R)]$. It is easy to show that the scaling law in eq. (1) follows if the probability density function $P(V(R))$ has the above mentioned scaling form.

The above equations for $g(t)$ have quite general validity. They hold, for example, even if the fluid is stationary, and the seed particles are undergoing Brownian motion only. In that case, $V(R)$ is independent of R and $P(V(R))$ is a Gaussian function. Then the function $G(t)$ is an exponentially decaying function [5], $G(t) = \exp(-2Dk^2t)$, where D is the diffusivity of the Brownian particles, and is given by Stokes' law. This contribution to the decay of $G(t)$ will be present, even when the fluid is turbulent. However, in a turbulent fluid, the decay time T of $G(t)$ is much shorter than the diffusive decay time, $T_d = 1/2Dk^2$, so that the latter contribution can be

safely ignored. From eq. (5), it follows that the turbulent decay time should be of the order of $T = 1/ku(L)$, because the fastest decay rate is associated with the largest eddies of size L.

3. Results

Over a wide range of slit widths and Reynolds numbers, we find that the function $G(t)$ exhibits the scaling form,

$$G(kt, L, \text{Re}) = G(\kappa) , \tag{6}$$

with $\kappa \sim k^\mu L^\zeta t$. This scaling behavior of $G(t)$ is observed only when the Reynolds number exceeded a certain value Re_c. In the case of the grid flow described above, Re_c was roughly 500, which corresponds to much weaker turbulence than that one normally associates with scaling behavior. It is quite possible that the scaling behavior is seen at such small values of Re because the simultaneous velocity difference $V(R)$ is measured and no frozen turbulence assumption is needed in the data analysis.

The exponent μ in eq. (6) was measured as follows. For a fixed slit width L and a fixed Re, $G(t)$ was measured at several scattering angles and hence several values of k. All of the plots of log $[G(t)]$ versus $\log(t)$ could be superimposed by horizontal translation of one graph with respect to another. The amount of translation, $\delta(k)$, is found to be roughly proportional to k, i.e. $\mu = 1$, when Re exceeded the critical value Re_c. However, in the absence of flow, $\mu = 2$, as expected for Brownian motion of the seed particles. Similar measurements were made in which k and Re were held fixed, and L was varied. Again all the plots of $\log[G(t)]$ versus $\log(t)$ could be superimposed, yielding the result $\kappa \sim kL^\zeta t$, as long as Re exceeded Re_c. In these experiments, ζ is found to be Re dependent. We return to this important observation below.

Fig. 2, a log–log plot of $G(\kappa)$ versus κ, shows the scaling behavior of $G(t)$ discussed above. The measurements correspond to several values of scattering angle, or k-value, several slit widths and at various

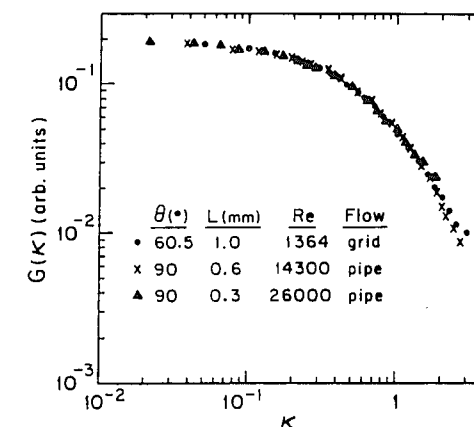| θ(°)	L (mm)	Re	Flow
• 60.5	1.0	1364	grid
x 90	0.6	14300	pipe
▲ 90	0.3	26000	pipe

Fig. 2. The scaling function $G(\kappa)$ versus $\kappa = qu(L)t$ in pipe flow and grid flow.

Reynolds numbers. In one set of measurements (closed circles), the grid was present; in the other two sets (crosses and triangles), the grid was removed (pipe flow). The correlation functions $G(t)$ have been horizontally (and vertically) translated so that they coincide. In the pipe flow measurements, the Reynolds number is based on the pipe diameter, making it an order of magnitude larger than that for the grid flow, even when the mean flow velocities U are comparable in both cases.

An alternative way to determine the exponent ζ was to plot, on a double logarithmic scale, the slit-width dependence of the decay time, T, of $G(t)$, keeping Re and k fixed. As is shown in fig. 3, linear variation of $\log(T)$ with $\log(L)$ was seen at intermediate values of L. The data in fig. 3 were obtained in the grid flow at three different Reynolds numbers Re = 460, 1400, and 2200. Since $T \approx 1/ku(L)$ and $u(L) \sim L^\zeta$, the slope of this line yields the exponent ζ, which is 1/3 in the Kolmogorov theory. We have verified that the power law behavior at large L was limited by the outer scale, l_0, of the turbulence. At small values of L the beam diameter was no longer negligibly small, which could account for the decrease in T at small values of L. Imperfections in the optical system may also be responsible for the decrease in T at small slit widths.

The behavior of $T(L)$ at small L has more recently been reexamined in a water tunnel of much superior
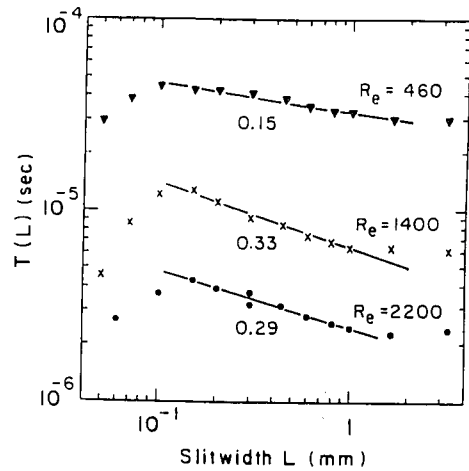
Fig. 3. The decay time $T(L)$ versus slit width L in grid flow. The number below a line is the slope of that line.

design to that used in the studies reported above. In this experiment, the optically transparent pipe, where $g(t)$ was measured, was square in cross section, rather than cylindrical, so that the laser beam was undistorted in passing through it. In this square pipe, the beam diameter was less than 0.1 mm, which is smaller than the smallest value of L at which $g(t)$ was measured. Using laser Doppler velocimetry and invoking the frozen turbulence assumption one can determine the smallest eddy size l_d. At Re=850, we obtained $l_d=0.4$ mm. At values of L between 0.4 mm ($=l_d$) and 0.1mm, the decay time of $G(t)$ became independent of L, i.e. $\zeta \approx 0$ when $L < l_d$. This result is very different from the Kolmogorov prediction, $\zeta = 1$ when $L < l_d$.

From the straight-line segment (solid line in fig. 3) we can extract the slope ζ which shows a Re-dependent feature. Fig. 4 shows ζ as a function of Re for both pipe flow and grid flow (insert). The exponent ζ is seen to increase from 0 to $\approx 1/3$ (the Kolmogorov value) as Re is increased. When the Reynolds number is below Re_c, $G(t)$ fails to exhibit scaling behaviour. The measured $Re_c \approx 300$–400 in the grid flow and $Re_c \approx 3000$–4000 when the grid was removed. Measurements in the improved water tunnel give similar results. These observations are consistent with
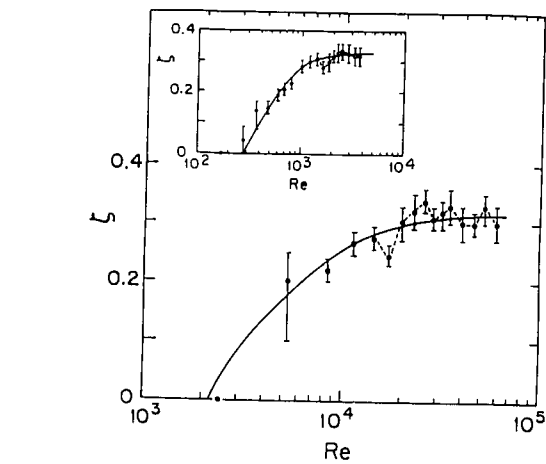

Fig. 4. The exponent ζ as a function of Re in pipe flow. The solid line is drawn by eye through the data points, and the dashed curve shows the oscillatory behavior of ζ. The inset shows ζ versus Re in grid flow.
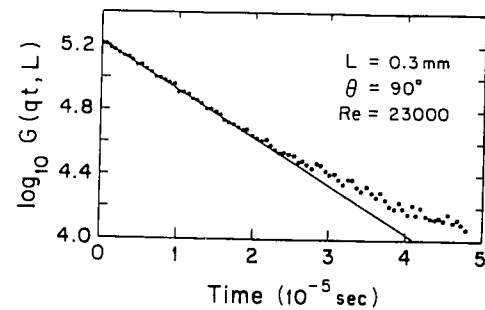

Fig. 5. A plot of $\log[G(qt, L)]$ versus t in pipe flow at indicated parameters.

the notion that the turbulence becomes increasingly three-dimensional as Re is increased above Re_c and that in the vicinity of Re_c, the turbulence is two-dimensional [9].

We now turn to the discussion about the functional form of $G(t)$. Fig. 5 is a semilog plot of $G(t)$ versus t in pipe flow at the indicated values of L, θ, and Re. The straight line is a linear fit to the data points at small t. It is seen that only at large time does the curve start to deviate from the linear behavior. If we assume that the characteristic function $F(ku(R)t)$ in eq. (5) has the form $F \sim \exp[-ku(R)t]$, $G(t)$ then

becomes an incomplete gamma function with $ku(L)t$ as its argument [8]. This equation is well fitted to our measurement of $G(t)$. An example of this good fit is shown in fig. 6. Note that the assumption of $F(x)$ being a single exponential decaying function implies that $P(V(R))$ is of Lorentzian form as shown in eq. (2). This function has a diverging second moment, to which the energy density in the fluid is proportional. Therefore $G(t)$ cannot have this form for large values of $V(R)$. We indeed observed departures from this Lorentzian form for $P(V(R))$ with very large values of $V(R)$ (corresponding to very small t for $G(t)$) [10,11]. However, these observations will not be discussed further here. Most theories of turbulence concentrate on the scaling behavior of the moments of $V(R)$, rather than in $P(V(R))$ itself. Quite often, $P(V(R))$ is assumed to be of Gaussian form, $P(V(R)) \sim \exp\{-[V(R)/u(R)]^2\}$, but this form of $P(V(R))$ is clearly contrary to our findings.

How can one understand that the exponent ζ increases from 0 to $\approx 1/3$ as the fluid becomes increasingly turbulent? A fundamental understanding of this result is lacking, but it can be said that the observation is consistent with the notion that the turbulent active region is a fractal [12]. Let the fractal dimension of the turbulent region be D. Since the turbulent energy is confined to active regions of dimension $D < 3$, the concentration of the turbulent energy is increased to smaller regions, relative to the case of volume-filling turbulence. Modifying the Kolmogorov
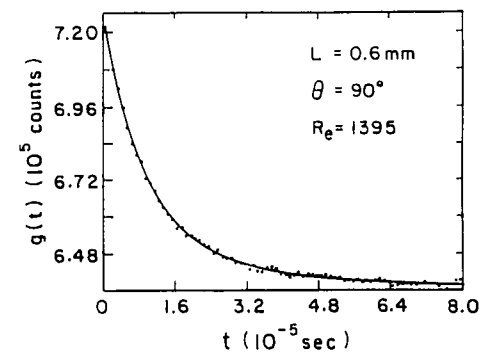
theory to take this effect into account [13], one has $u(R) \sim R^\zeta$, with $\zeta = \frac{1}{3}(1+D-3)$. According to this model, the increase of ζ from 0 to $\approx \frac{1}{3}$ corresponds to an increase of D from 2 to 3.

It should be stressed that our measurements of $g(t)$ described above, do not directly give information about the fractal dimension of the energy-containing eddies; it can only be said that the data invite such an interpretation. The above interpretation of the data in fig. 4 is supported by the recent work of Shreenivasan et al. [3]. They measured the fractal dimension of the interface of two counter-flowing fluids, one of which has been dyed. Such measurements, made in the vicinity of Re_c, support the conclusion that increasing Re above Re_c increases the dimensionality of the turbulent active region. With one adjustable parameter, Re_c, the data of Shreenivasan et al. can be directly superimposed on the measurements in fig. 4 [3].

Even if the energy-containing eddies in a turbulent field occupy regions with dimensionality less than 3, it is not necessary that the entire turbulent region be characterized by a homogeneous fractal. Benzi et al. [14] have proposed a model that the turbulent region is a multifractal object. In their model there is a probability, x, that the turbulent region is space filling ($D=3$) and a probability, $1-x$, that $D=2$. Our measurements are consistent with this model, provided one makes an additional assumption that x is a function of the Reynolds number. The details of the model have been worked out for a general function of $x(\mathrm{Re})$ and fitted to experiment [9]. At present, however, our measurements are not precise enough to confirm that a multifractal model is required to explain the observations.

4. Concluding remarks

What started out as a study carried out in the time domain (the measurement of $g(t)$), has ended up by yielding spatial information about turbulent flow. The homodyne experiments provide further confirmation of the notion of Mandelbrot that the energy-

Fig. 6. A typical autocorrelation function $g(t)$ versus t in grid flow. The solid line is a fit to the incomplete gamma function.

containing eddies are fractal in their geometrical structure. This finding is not new. What seems to have gone unnoticed before, is that the fractal dimension of the turbulence changes with changing Reynolds number, when some critical value of this parameter is exceeded. The interpretation of these experiments makes no appeal to the frozen turbulence assumption. By using the technique of photon correlation homodyne spectroscopy, we have been able to observe the self-similar behavior of turbulent flows at moderate Reynolds number that were heretofore regarded as too weak to exhibit universal features.

Acknowledgements

References

[1] B.B. Mandelbrot, The Fractal Geometry of Nature (Freeman, San Francisco, 1982).
[2] B. Mandelbrot, Phys. Fluids Suppl. 10 (1967) S302.
[3] K.R. Sreenivasan, R. Ramshankar and C. Meneveau, Proc. Roy. Soc. (London) A 421 (1989) 79.
[4] E.R. Lindgren, Arch. Fys. (1959) 97.
[5] B.J. Berne and R. Pecora, Dynamic Light Scattering (Wiley, New York, 1976).
[6] P.J. Bourke et al., J. Phys. A 3 (1970) 216.
[7] A.N. Kolmogorov, C.R. (Dokl.) Acad. Sci. URSS 30 (1941) 301; 31 (1941) 538.
[8] P. Tong et al., Phys. Rev. A 37 (1988) 2125; P. Tong and W.I. Goldburg, Phys. Fluids 31 (1988) 2841.
[9] P. Tong and W.I. Goldburg, Phys. Fluid 31 (1988) 3253.
[10] A. Onuki, Phys. Lett. A 127 (1988) 143.
[11] P. Tong and W.I. Goldburg, Phys. Lett. A 127 (1988) 147.
[12] B.B. Mandelbrot, J. Fluid Mech. 62 (1974) 331; in: Lecture Notes in Physics, Vol. 12. Statistical Models and Turbulence, M. Rosenblatt and C.W. Van Atta, eds. (Springer, Berlin, 1972), p. 333.
[13] U. Frisch, P. Sulem and M. Nelkin, J. Fluid Mech. 87 (1978) 719.
[14] R. Benzi et al., J. Phys. A 17 (1984) 3521.

ASYMMETRIC RANDOM WALK ON A RANDOM THUE–MORSE LATTICE ☆

S. GOLDSTEIN, K. KELLY, J.L. LEBOWITZ [1] and D. SZASZ [2]

Department of Mathematics, Rutgers University, New Brunswick, NJ 08903, USA

Dedicated to Benoit Mandelbrot on the occasion of his 65th birthday

We study the behavior of an asymmetric random walk in a one-dimensional environment whose nonuniformity is in between that of quasi-periodic and random. We construct the environment from arithmetic subsequences of the Thue–Morse sequence. The construction induces in a natural way a measure μ on the space of environments which is invariant and ergodic with respect to translations but is not mixing and has zero entropy. The behavior of the random walk is rather similar to that found by Sinai for the Bernoulli case, when μ is a product measure for which the entropy has its maximum value; i.e. the particle motion is subdiffusive, the displacement growing in time as $(\log t)^{1/\beta}$, $\beta = \log 3/\log 4$. The nature of the dramatic Sinai–Golosov "localization" is however quite different, exhibiting an interesting fractal structure whose nature depends upon the time scale of observation.

1. Introduction

We study the behavior of an asymmetric random walk in a one-dimensional environment whose nonuniformity is in between that of quasi-periodic and random. We will specify the environment by a "spin" configuration $\xi = \{\xi_j\}$, $\xi_j = \pm 1$, $j \in \mathbb{Z}$. Given ξ and some $0 < \epsilon < 1$, the random walk has a transition probability at site j to the right, p_j (and to the left, $1 - p_j$), of the simple form $p_j = \frac{1}{2}(1 + \epsilon \xi_j)$.

We will consider environments $\xi = \{\xi_j\}$ which are obtained from arithmetic subsequences of the Thue–Morse substitutional sequence [1,2], in a manner to be described in section 3. The construction will induce in a natural way a unique measure μ on the space of configurations (possible environments) $\{-1, 1\}^{\mathbb{Z}}$ [2]. This measure μ is invariant and ergodic with respect to translations but is not mixing, and has zero entropy.

We shall later see that despite this lack of randomness in the environment, the behavior of the random walk is rather similar to that found by Sinai [3] for the Bernoulli case, when μ is a product measure for which the entropy has its maximum value; i.e. the particle motion is subdiffusive, the displacement growing as a power of a logarithm in time. To see how this comes about we now discuss briefly the general setting of the Sinai theorem, while retaining the simple relation $p_j = \frac{1}{2}(1 + \epsilon \xi_j)$.

In one dimension it is always possible to define a potential energy function $U(j)$ so that the transition probabilities satisfy the detailed balance condition with respect to the (non-normalized) measure $\exp[-U(j)]$, i.e.

$$p_j / (1 - p_{j+1}) = \exp[U(j) - U(j+1)]. \tag{1}$$

Hence the measure $\exp[-U(j)]$ is stationary. Also, it follows that for a translation-invariant ergodic measure μ on the ξ_j, the condition of no drift is simply $\langle \xi_j \rangle_\mu = 0$.